Evaluation of load transfer characteristics of five different implants in compact bone at different load levels by finite element analysis

Dinçer Bozkaya[1], MS
Graduate Student

Sinan Müftü[1,3], MS, PhD
Associate Professor

Ali Müftü[2], DMD, MS, PhD
Assistant Professor

[1]Northeastern University
Department of Mechanical Engineering
Boston, MA 02115

[2]Tufts University
Department of Restorative Dentistry
School of Dental Medicine
Boston, MA 02111

November, 2003

Support information: The work of DB and SM during this research was, in part, supported by Bicon, Inc., Boston, MA through a research grant to Northeastern University.

[3] Corresponding author: E-mail: smuftu@coe.neu.edu, Phone/Fax: (617) 373-4743/2921

ABSTRACT

Statement of problem. Load transfer characteristics of dental implants depend on implant geometry as well as the level of external load applied on the implant. Considering the wide range of implant applications, and number of implant designs on the market, better understanding of the effect of macroconfiguration on stress distribution is an important issue for clinical success.

Purpose. Load transfer characteristics of five commercially available dental implant systems were compared.

Materials and Methods. Five different implant systems comparable in size, but different in thread profile and in crest module shapes were compared using the finite element method. Bone quality-II was approximated and full osseointegration was assumed. Occlusal loads of varying magnitudes were applied on the abutments, at 11.3^{o} from the vertical axis with a 1 mm offset. Total overloaded bone area, where tensile and compressive normal stresses fall outside of their safe limits of 100 and 170 MPa, respectively, was investigated for different load levels.

Results. For moderate levels of occlusal loads up to 300 N, the compact bone was not overloaded by any one of the implant systems. For the extreme end of the occlusal load range (1000 N or more) the overloading characteristics of implants depend strongly on their geometric shape.

Conclusion. In general, overloading occurs near the top region of the compact bone, in compression, and it is primarily caused by the normal and lateral components of the occlusal load. At the intersection region of the compact with the trabecular bone, overloading occurs in tension due to the vertical component of the occlusal load. For

excessive forces greater than 1000 N, the overloaded areas of the bone vary considerably among five different implants.

Clinical Implications

Overload due to excessive forces could lead to bone weakening or loss. The shape of the crestal module could play a significant role in minimizing the bone overload.

1. INTRODUCTION

Endosseous dental implants are currently used to retain and/or support prostheses for a variety of tooth loss scenarios. The traditional undisturbed healing concept has been proven to be very successful long-term for both one[1,2] and two-stage[3,4] implant placement protocols. Recently, promising results have also been observed for select cases when implants were subjected to immediate functional loads[5-7]. Whether an implant is placed in function following a certain period of undisturbed healing or immediately after placement, likelihood of osseointegration and prognosis thereafter, are greatly influenced by the biomechanical environment. Factors that affect the load transfer at the bone-implant interface include the type of loading, material properties of the implant and prosthesis, implant geometry, surface structure, quality and quantity of the surrounding bone, and nature of the bone–implant interface[8]. Currently, there are more than 50 implant designs available in the market. The evolution has been by way of incremental changes in size, shape, materials and surfaces of earlier designs, driven, at times, by market demands rather than basic science research[9]. Considering the expanded indications for implants and changing clinical protocols, the relation between implant design and load distribution at the implant-bone interface continues to be an important issue.

From an engineering stand point, an important issue is to design the implant with a geometry that will minimize the peak bone stress caused by standard loading[10]. The complex geometry of the implants prevents the use of closed form solutions in stress analysis. The finite element (FE) method has been applied to the dental implant field to compare stress distribution patterns in the implant-bone interface not only by comparison

of various root-form implant designs[10-15], but also by modeling various clinical scenarios [16-19] and prosthesis designs[20-23]. This method offers the advantage of solving complex structural problems by subdividing them into smaller and simpler interrelated sections by using mathematical techniques[8,15].

FE analyses, which investigate the relation between implant design and stress distribution, have addressed the overall shape and size of the implant body, implant neck geometry and thread geometry for threaded implants. Rieger et al.[12] showed that a tapered design made of a material with high elastic modulus would be most suitable to serve as a free-standing implant. Siegele and Soltesz[13] demonstrated significant variations in stress distributions in the bone under a vertical load where implant surfaces with very small radii of curvature or geometric discontinuities, such as steps, exhibited higher stresses than smoother shapes, such as cylinders or screws. They also showed that lateral loading caused maximum stress concentration in the region of direct-implant bone contact and soft tissue layer for the cylindrical implants and below the uppermost thread for the screw-type implant. Holmgren et al. [15] suggested considering application of oblique load to FE analysis, indicating that these were more realistic bite directions capable of causing the highest localized stress in the cortical bone. These authors found the stepped design to exhibit a more even stress pattern than a straight cylindrical design.

Threaded implants exhibit geometric variations in terms of thread pitch, shape and depth. Threads function to provide initial stability and to increase surface area of the implant. Use of different thread configurations for different bone qualities have been proposed as thread geometry could play an important role in the type of force transmitted[25-28]. Recently, Chun et al. applied the FE method to find the optimal thread

design[29]. Under a 100 N oblique load of 15°, the maximum stress in compact bone was found to be higher for the plateau design compared to the triangular or square designs and their variations. According to these authors, screw pitch had a significant impact on the stress distribution. Patra et al. [30] reported that a tapered thread design implant exhibited higher stress levels in bone than the parallel profile thread.

The transosteal region of the implant body has been defined as the 'crest module'[24]. For most systems, this neck portion of the implant is smooth. Different designs include parallel, converging and diverging sides. One particular implant investigated by Hansson[10] using the FE method included both a taper and retention elements all the way up to the crest and was found to have much lower interfacial shear stresses compared to a smooth neck design.

The purpose of this study is to evaluate the stress transfer properties of five currently marketed implants that differ significantly in macroscopic geometry. In order to perform this task, five systems are evaluated under increasing load levels using the FE method. This approach allows, not only the evaluation of load transfer characteristics under regular chewing forces, but also under the extreme load levels, such as those that occur during parafunction. The comparison is carried out in the compact bone with a new comparison criterion; the *overloaded area* in the compact bone is defined as the area where the principle stresses exceed the allowable tensile and compressive strength of the bone. In general, the extent of the overloaded area increases with increasing external (biting) loads. In what follows the load transfer characteristics of particular implant designs are shown to have a significant effect on how the overload area grows with increasing loads.

2. MATERIALS AND METHODS

In this study five commercially available dental implants are compared. The details of the selected implant systems from Ankylos (Degussa Dental, Hanau-Wolfgang, Germany), Astra (Astra Tech AB, Mölndal, Sweden), Bicon (Bicon Inc., Boston, MA, USA), ITI ITI (Institut Straumann AG, Waldenburg, Switzerland) and Nobel Biocare (Nobel Biocare AB, Göteborg, Sweden) are given in Table 1. The diameters and heights of implants are selected to be comparable in size. The thread profiles and the shapes of the crestal modules of the implants are different as shown in Figure 1. Abutment heights are adjusted to allow the load application at the same height with respect to the bone. The diameter of the implants, length of the implant in the bone and the surface area of the implant in the bone, for all the implants considered here, are given in Table 2.

2.1 The Finite Element Model

Three dimensional (3D) CAD models of the implants and abutments were created using Pro/Engineer 2001 as shown in Figure 1. Care was taken to use a very fine FE mesh to represent the model of the implants and the bone. In general, increasingly fine mesh size ensures convergence of a FE solution[34]. Use of large number of elements is especially important in this problem, where stress singularities are expected at the sharp corners, (marked with arrows in Figure 1) of the solution domain. The number of elements and nodes used in this study are given in Table 3. Axisymmetric FE models are constructed for all implant-abutment-bone systems, in Ansys 6.1 (Ansys Inc., Houston, Pennsylvania, USA). The axisymmetric approach, where a cross-section can be meshed with large number of elements, provides optimal use of computing resources. The

implants and abutments are modeled as Ti6Al4V with linear-elastic, isotropic and homogenous properties. The Young's modulus and the Poisson's ratio of the titanium alloy are 114 GPa and 0.34, respectively[36].

The bone is modeled as a cylinder with 20 mm diameter and 22 mm height around the implant. The cortical bone is modeled at the top and bottom of the cylinder as 2 and 3 mm thick layers, respectively, with an elastic modulus of 13.7 GPa. The trabecular bone is modeled as a 17 mm thick layer between two cortical layers, with an elastic modulus of 1 GPa. These properties approximate the bone as quality-II bone. Implant-to-bone contact was assumed to be 100 per cent, indicating perfect osseointegration.

2.2 The Criterion for Bone Overload

In the broadest sense, bone failure can be defined as local fracture of the bone due to excessive local loads. The mechanical properties of the *cortical bone* depends on several factors such as the porosity of the bone, mineralization level, bone density, collagen fiber organization, and rate of deformation[37]. Moreover, the cortical bone is typically anisotropic. The ultimate stress of the cortical bone has been reported to be higher in compression (170 MPa) than in tension (100 MPa). The mechanical properties of the *trabecular bone* depend on porosity, the anisotropy of the trabecular architecture and material properties of the tissue in the individual trabeculae. The strength of the trabecular bone has been reported to be the same in tension and compression, and its value is on the order of 2-5 MPa[37].

It can be argued that bone resorption is also a failure mode, however, it takes place over a longer time period. It has been hypothesized that the strain in the bone tissue stimulates the biological response resulting in resorption (and remodeling) in the bone. The physiologic loading zone has been reported to be in the 1000-3000 microstrain range[38].

Here we study the localized bone failure due to fracture. The strain distribution will be the topic of another paper. We use the *maximum normal (principal) stress criterion* to predict local bone failure, which states that the material will fail when the maximum normal stresses at a point exceeds the maximum allowable normal stress[35]. Thus this criterion provides a way to identify failure regions due to tensile and compressive failure.

The maximum normal stress criterion is implemented as follows. Distribution of maximum normal stresses in the bone is calculated by the FE method. The regions where the maximum principle stresses (tensile) are greater than 100 MPa and the minimum principle stresses (compressive) are greater than 170 MPa are identified; and, the corresponding bone areas of these regions are calculated. In these localized regions the bone is declared as overloaded, and it is likely to fail.

It should be emphasized that the overload area method introduced here is only used as a qualitative comparison metric for different implant systems. Otherwise, it will be seen later in the paper that the extent of the overload area is minimal, due to a single incidence of excessive overloading. However, the overloaded regions are found to be curiously close to the crestal region of the compact bone, which may explain why some systems are more vulnerable to crestal bone loss. Successive over loading may spread the

failure pattern to significant levels, and the volume of bone that carries the load could decrease due to resorption. Note that bone remodeling is beyond the scope of this paper.

2.3 Loads

The forces exerted on an abutment vary in direction and magnitude. On a single tooth or implant, the largest forces occur along the axial direction. The axial loads have been measured to vary between 77 and 2440 N[33]. Generally, the lateral component of the occlusal force is significantly smaller and considered to be less than 100 N[33]. In this work, three types of loads were applied to the abutment to simulate different loading conditions that can be seen during mastication or biting in implants that carry single tooth or fixed prosthesis. These are vertical (F_V) and lateral (F_L) loads applied on the vertical axis of the implant, and bending moments (M). These loads are subsequently superposed to represent the effect of the occlusal load (F_O). By investigating the effects of the components, which ultimately become the occlusal force, upon superposition, we can identify the details of the load transfer mechanisms of the different implants.

Figure 2 gives a schematic depiction of the loads. Note that F_L and M are non-axisymmetric. They are applied to our axisymmetric model by expressing the load in Fourier series in terms of circumferential coordinate variable[34]. For this purpose, the geometry is discritized by, Plane 25, 4-noded axisymmetric harmonic elements in Ansys. Once a solution is found the post processing software allows calculation of the stress distribution at any circumferential cross-section. In this work the following ranges were used: $0 < F_V < 2500$ N; $0 < F_L < 500$ N; $0 < M < 4000$ N.mm; and $0 < F_O < 2000$ N. The occlusal loads are applied 1 mm off center from the vertical axis of the implant with 11.3^o

inclination as shown in Figure 2. The pure vertical and tangential loads and bending moments are applied on the vertical axis.

3. RESULTS

The effects of external loading on the growth of overload area for five different implant systems are presented next. The area of the overloaded compact bone is calculated in the cross-section directly opposite of the loads, as shown in Figure 2, where the stresses are maximum. The variation of overloaded area of the bone as a function of vertical loads, lateral loads, bending moments and occlusal loads are presented in Figure 3a-d, respectively. Distribution and location of the overloaded areas in the compact bone for each implant system are presented in Figure 4. As mentioned above, the predicted regions of overloaded compact bone, presented next, are for instantaneous loads and do not represent the effect of loading history.

3.1 Bone Overload Due to Vertical Loads

Figure 3a shows the overloaded area estimated as a function of the vertical load F_V. The bone overload area is not significant up to a load of 1800 N in all implants; however, it grows with an increasing rate after this load. Generally, the amount of bone overload area of ITI implant is higher than the other implant designs. The other systems show comparable levels of overload area.

The details of bone overload patterns due to the maximum normal stress criterion are shown in Figure 4a, for a vertical load of 2500 N. This figure shows high compressive stresses at the crestal region of the bone and high tensile stresses at the intersection region

of the implant, cortical bone and trabecular bone. No significant overload is found in Ankylos and Bicon implants due to compressive stresses near the top of the crestal module. The compressive and tensile stresses are comparable within the other group for Astra, ITI and Nobel Biocare implants, where the overloaded area in tension is larger than the overloaded area in compression. The bone overload in the crestal region is higher in Astra, ITI and Nobel Biocare implants due to the high compressive stresses.

3.2 Bone Overload Due to Lateral Loads

The variation of the bone overload area as a function of lateral load F_L is presented in Figure 3b. This figure shows that the ITI system reaches a 0.05 mm^2 area of overloaded bone when the lateral load is approximately 400 N. This level of overloaded area for the other implant systems occurs when F_L > 500 N. The predicted bone overload is highest in the ITI system and lowest in the Ankylos system.

The details of the bone overload patterns of the implants due to a lateral load of 500 N are presented in Figure 4b. This figure shows that high compressive stresses occur at the top of the crestal region of the bone and high tensile stresses occur at the intersection of implant, cortical bone and trabecular bone. Overload occurs at the top of the crestal bone for Astra, ITI and Nobel Biocare implants. Bone overload is more likely to be due to tensile stresses occurring at the intersection of implant, cortical and trabecular bone for the Bicon implant; and, compressive stresses also occur near the tip of the implant as the load is increased. No significant amount of bone overload is predicted at the crestal region of the Ankylos implant.

3.3 Bone Overload Due to Bending Moments

The variation of the bone overload area as a function of bending moment M is presented in Figure 3c. The overloaded area is predicted to be the largest for the ITI system, whereas Astra, Bicon and Nobel Biocare systems show comparable amounts of bone overload. The Ankylos system shows no significant amount of bone overload.

The details and distribution of overloaded bone areas in the crestal compact bone are shown in Figure 4c, for a bending moment of 4000 N.mm. This shows that the bending moment (applied as shown in Figure 2) creates tensile stresses near the crestal region of the cortical bone, and no compressive stress region with significant magnitude exists. The amount of bone failure area in Ankylos implant is negligible and the other implants show more than 0.05 mm^2 bone loss at this level of bending moment.

3.4 Bone Overload Due to Occlusal Loads

The variation of the bone overload area as a function of occlusal load F_O is presented in Figure 3d. The occlusal loads are applied at an inclination of 11.3^o, measured from the longitudinal axis of the implant, and they are offset by 1 mm from the central axis. This figure shows that the bone overload area remains under 0.05 mm^2 up to a load of 1200 N. The calculated bone overload is quite comparable amongst the five systems, however the highest one occurs in the ITI implant. The Astra, Bicon and Nobel Biocare implants show similar variation of bone overload with increasing load magnitude.

Details of the bone overload patterns due to an occlusal load with a magnitude of 1632 N are shown in Figure 4d. High compressive stresses occur at the top of the crestal region of the bone, whereas high tensile stresses are found at the intersection of the

implant, cortical bone and trabecular bone. Bone overload in compression is estimated at the top of the crestal region for Astra, ITI and Nobel Biocare implants. This is in addition to the tensile overload at the intersection region, especially for ITI and Astra systems. In Ankylos and Bicon implants, the bone overload is more likely to be due to tensile stresses occurring at the intersection of the implant, cortical and trabecular bone; and, no bone overload is observed at the top of the crestal region.

4. DISCUSSION AND CONCLUSIONS

In this work the effect of external forces on bone overload is investigated for different implant systems using the FE method. The maximum normal stress criterion is used to evaluate the extent of the regions where the normal stresses are beyond the allowable tensile (100 MPa) and compressive (170 MPa) values in the cortical bone. It is found that *occlusal load, F_O,* does not cause large overload regions up to load magnitudes of 1000-1200 N (Figure 3d and Figure 4d).

Near the *top of the compact bone*, no overload is observed for the Ankylos and Bicon systems; however, overload regions in compression are found for Astra, ITI, and Nobel Biocare systems. The extent of the overloaded regions in the compact bone agrees with the histomorphogical studies that show the early bone loss in the crestal region. It should be noted that the crestal modules of Ankylos and Bicon systems have a narrowing shape, where as the shape of the other three implants in this region are either straight or widening as shown in Figure 1. This suggests that implants with narrowing cross-sections at the top of the cortical bone create more favorable load transfer characteristics for single tooth implants, in this region.

At the *intersection region* of the trabecular bone, cortical bone and the implant all implants eventually develop maximum tensile stresses above 100 MPa, at high levels of external (biting) loads. In this region, Ankylos implant develops the least amount of overload area followed by Nobel-Biocare, Bicon and Astra with comparable values; the ITI system shows the largest overload area. The tensile overload in this region is primarily due to the vertical component of the load F_V, (Figure 4a) and it develops regardless of the local geometry of the implant in this region. However, the overloaded area is greater in the intersection region for the four implants, which have screw threads or fins in this region.

In summary, this work shows that for moderate levels of occlusal loads (100-300 N), applied at 11.3^o from the vertical axis with a 1 mm offset, the compact bone is not overloaded by any one of the implant systems investigated here. For the extreme end of the occlusal load range (1000 N or more), i.e. in case of parafunction, the overloading characteristics of different implants depend strongly on the geometric shape. In general, overloading occurs near the top region of the compact bone, in compression; and, it is primarily caused by the normal and lateral components of the occlusal load. At the intersection region of the compact and trabecular bones, overloading occurs in tension; and, it is primarily due to the vertical component of the occlusal load.

Acknowledgements

Two of the authors, DB and SM, would like to acknowledge the partial support of Bicon, Inc., Boston, MA, USA, for this work. The authors would also like to thank Mr. Fred Weekley (United Titanium, Wooster, OH, USA) and Mr. Paulo Coelho, D.M.D. (University of Alabama, Birmingham, AL, USA) for their insightful comments.

List of Tables

List of Figures

REFERENCES

1. Ferrigno N, Laureti M, Fanali S, et al. A long-term follow-up study of non-submerged ITI implants in the treatment of totally edentulous jaws. Part I: Ten-year life table analysis of a prospective multicenter study with 1286 implants. *Clin Oral Implants Res*. 2002; 13(3):260-273.
2. Romeo E, Chiapasco M, Ghisolfi M, Vogel G, Long-term clinical effectiveness of oral implants in the treatment of partial edentulism. Seven-year life table analysis of a prospective study with ITI dental implants system used for single-tooth restorations. *Clin Oral Implants Res.* 2002;13(2):133-143.
3. Adell R, Lekholm U, Rockler B, Branemark PI. A 15-year study of osseointegrated implants in the treatment of the edentulous jaw. *Int J Oral Surg*. 1981;10(6):387-416.
4. Adell R, Eriksson B, Lekholm U, Branemark PI, Jemt T. Long-term follow-up study of osseointegrated implants in the treatment of totally edentulous jaws. *Int J Oral Maxillofac Implants.* 1990;5(4): 347-359.
5. Ericsson I, Nilson H, Lindh T, Nilner K, Randow K. Immediate functional loading of Branemark single tooth implants. An 18 months' clinical pilot follow-up study. *Clin Oral Implants Res.* 2000:11(1);26-33.
6. Branemark PI, Engstrand P, Ohrnell LO, Grondahl K, Nilsson P, et al. Branemark Novum: a new treatment concept for rehabilitation of the edentulous mandible. Preliminary results from a prospective clinical follow-up study. *Clin Implant Dent Relat Res*. 1999:1(1);2-16.
7. Chow J, Hui E, Liu J, Li D, Wat P. The Hong Kong Bridge Protocol. Immediate loading of mandibular Branemark fixtures using a fixed provisional prosthesis: preliminary results. *Clin Implant Dent Relat Res*. 2001:3(3);166-174.
8. Geng JP, Tan KB, Liu GR. Application of finite element analysis in implant dentistry: a review of the literature. *J Prosthet Dent*, 2001:85(6);585-598.
9. Brunski JB. In vivo bone response to biomechanical loading at the bone/dental-implant interface. *Adv Dent Res*. 1999:13;99-119.

10. Hansson S. The implant neck: smooth or provided with retention elements: A biomechanical approach. *Clinical Oral Implants Research*, 1999:10(5);394-405.
11. Rieger MR. Finite element stress analysis of root-form implants. *J Oral Implantol*, 1988:14(4); 472-484.
12. Rieger MR, Adams WK, Kinzel GL, Brose M. Bone stress distribution for three endosseous implants. J Prosthet Dent. 1989: 61(2); 223-228.
13. Siegele D, Soltesz U. Numerical investigations of the influence of implant shape on stress distribution in the jaw bone. *Int J Oral Maxillofac Implants.* 1989:4(4);333-340.
14. Rieger MR, Adams WK, Kinzel GL. A finite element survey of eleven endosseous implants. *J Prosthet Dent*, 1990:63(4);457-465.
15. Holmgren EP, Seckinger RJ, Kilgren LM, Mante F. Evaluating parameters of osseointegrated dental implants using finite element analysis--a two-dimensional comparative study examining the effects of implant diameter, implant shape, and load direction. *J Oral Implantol*. 1998:24(2);80-88.
16. Akca K, Iplikcioglu H. Finite element stress analysis of the influence of staggered versus straight placement of dental implants. *Int J Oral Maxillofac Implants*, 2001:16(5);722-730.
17. Iplikcioglu H, Akca K. Comparative evaluation of the effect of diameter, length and number of implants supporting three-unit fixed partial prostheses on stress distribution in the bone. *J Dent*. 2002:30(1);41-46.
18. Pierrisnard L, Hure G, Barquins M, Chappard D. Two dental implants designed for immediate loading: a finite element analysis. *Int J Oral Maxillofac Implants.* 2002:17(3);353-362.
19. Van Oosterwyck H, Duyck J, Vander Sloten J, Van Der Perre G, Naert I. Peri-implant bone tissue strains in cases of dehiscence: a finite element study. *Clin Oral Implants Res*. 2002:13(3);327-333.
20. Papavasiliou G, Kamposiora P, Bayne SC, Felton, D. Three-dimensional finite element analysis of stress-distribution around single tooth implants as a function of bony support, prosthesis type, and loading during function. *J Prosthet Dent*. 1996:76(6);633-640.

21. Papavasiliou G, Tripodakis AP, Kamposiora P, Strub JR, Bayne S. Finite element analysis of ceramic abutment-restoration combinations for osseointegrated implants. *Int J Prosthodont*, 1996:9(3);254-260.
22. Stegaroiu R, Kusakari H, Nishiyama S, Miyakawa O. Influence of prosthesis material on stress distribution in bone and implant: a 3-dimensional finite element analysis. *Int J Oral Maxillofac Implants*, 1998:13(6);781-790.
23. Stegaroiu R, Sato T, Kusakari H, Miyakawa O. Influence of restoration type on stress distribution in bone around implants: a three-dimensional finite element analysis. *Int J Oral Maxillofac Implants*. 1998:13(1);82-90.
24. Misch CE. *Contemporary implant dentistry*. 2nd ed. 1999, St. Louis: Mosby. xviii, 684.
25. Misch CE, Bidez MW, Sharawy M. A bioengineered implant for a predetermined bone cellular response to loading forces. A literature review and case report. *J Periodontol*, 2001:72(9);1276-1286.
26. Misch CE, Dietsh-Misch F, Hoar J, Beck G, Hazen R, et al. A bone quality-based implant system: first year of prosthetic loading. *J Oral Implantol*. 1999:25(3);185-197.
27. Misch CE, Hoar J, Beck G, Hazen R, Misch C. M. A bone quality-based implant system: a preliminary report of stage I & stage II. *Implant Dent*, 1998:7(1);35-42.
28. Misch CE. Implant design considerations for the posterior regions of the mouth. *Implant Dent*. 1999:8(4);376-386.
29. Chun HJ, Cheong, SY, Han JH, Heo, SJ, Chung, JP, et al. Evaluation of design parameters of osseointegrated dental implants using finite element analysis. *J Oral Rehabil*. 2002:29(6);565-574.
30. Patra AK, DePaolo JM, D'Souza KS, DeTolla D, Meenaghan M. Guidelines for analysis and redesign of dental implants. *Implant Dent*. 1998:7(4);355-68.
31. Geng J, Tan, KBC, Liu G. Application of finite element analysis in implant dentistry: a review of literature. *J Prosthet Dent*. 2001:85;585-598
32. Akca K, Iplikcioglu H. Finite element stress analysis of the effect of short implant usage in place of cantilever extensions in mandibular posterior edentulism. *Journal of Oral Rehabilitation*; 2002:29;350-356

33. Brunski JB. Biomechanics of Dental Implants. In eds. Block, M., Kent, J.N. and Guerra LR. *Implants in Dentistry*. Philadelphia, Pa, W.B. Saunders Co;1997:63-71.
34. Cook RD, Malkus DS, Plesha ME. *Concepts and Applications of Finite Element Analysis*. John Wiley & Sons, New York, NY;1989.
35. Mendelson, A. *Plasticity: Theory and Application*. MacMillan, New York, NY; 1968.
36. Lemons JE, Dietsh-Misch F. Biomaterials for Dental Implants. In ed. Misch, CE *Implant Dentistry*. Mosby, St. Louis, MO; 1999.
37. Martin RB, Burr DB, Sharkey, NA. *Skelatal Tissue Mechanics*. Springer, New York, NY. 1998;127-178.
38. Rigsby DF, Bidez MW, Misch CE. Bone Response to Mechanical Loads; in ed. Misch CE. *Implant Dentistry*. Mosby, St. Louis, MO;1999.
39. Barber JR. *Elasticity,* Kluwer Academic Publishers. Dordrecht, The Netherlands; 1992.

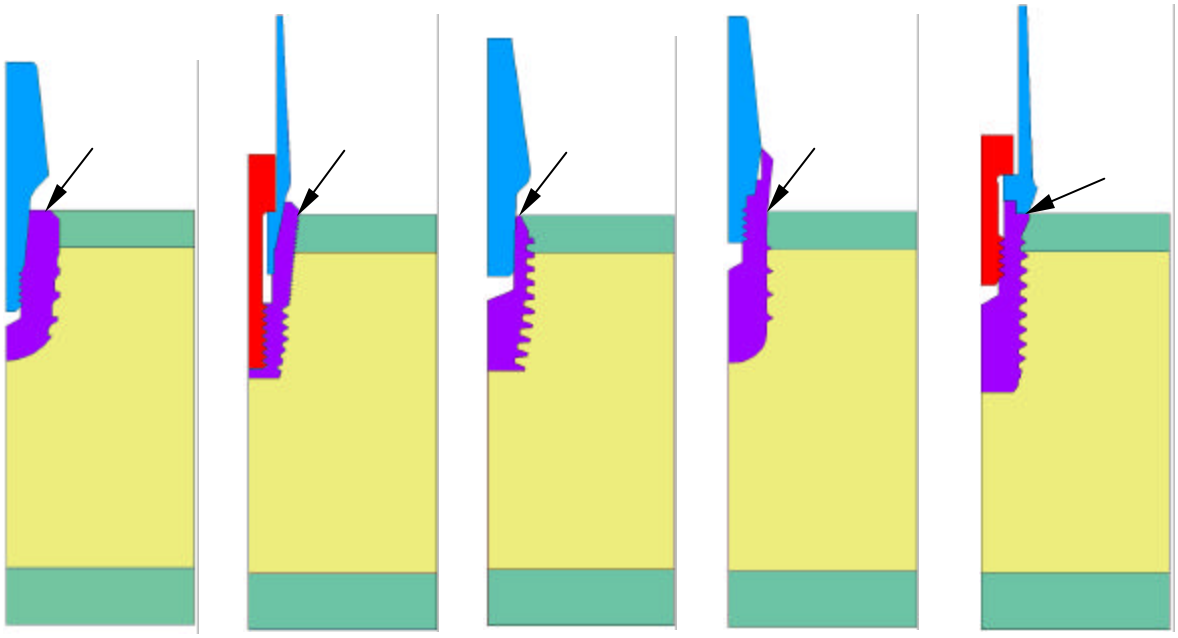

Ankylos Astra Bicon ITI Nobel Biocare

Figure 1 The axisymmetric CAD models of the bone and the five implant systems used in this study. The arrows indicate where high stress concentrations are expected based on theory of elasticity.

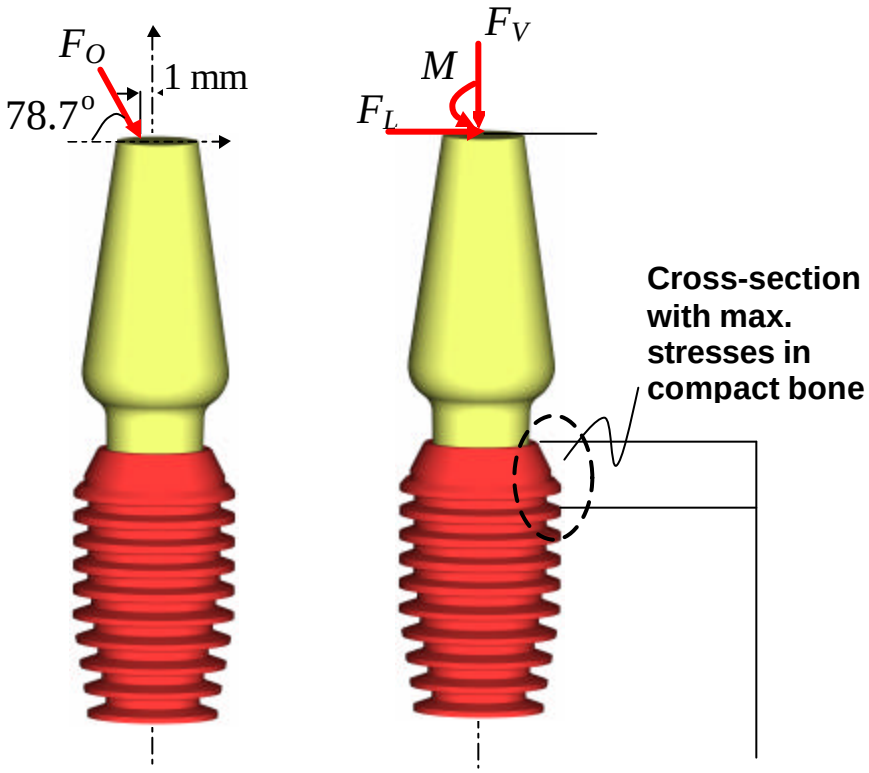

Figure 2 Description of the loads used in the study.

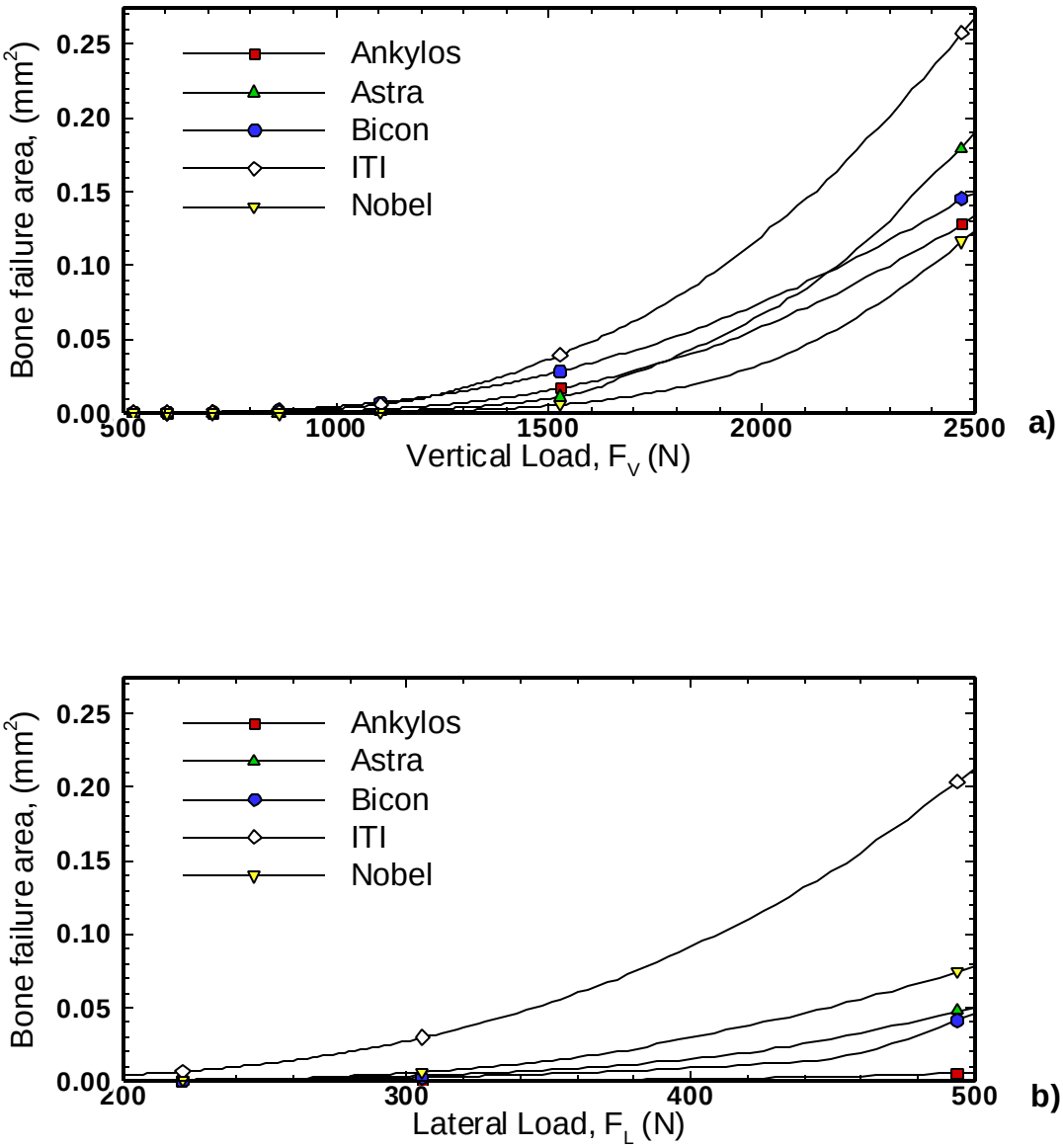

Figure 3. Predicted amount of bone failure area as a function of load magnitude for a) vertical load, b) horizontal load, c) bending moment, and d) occlusal load, for the five implant systems used in the study.

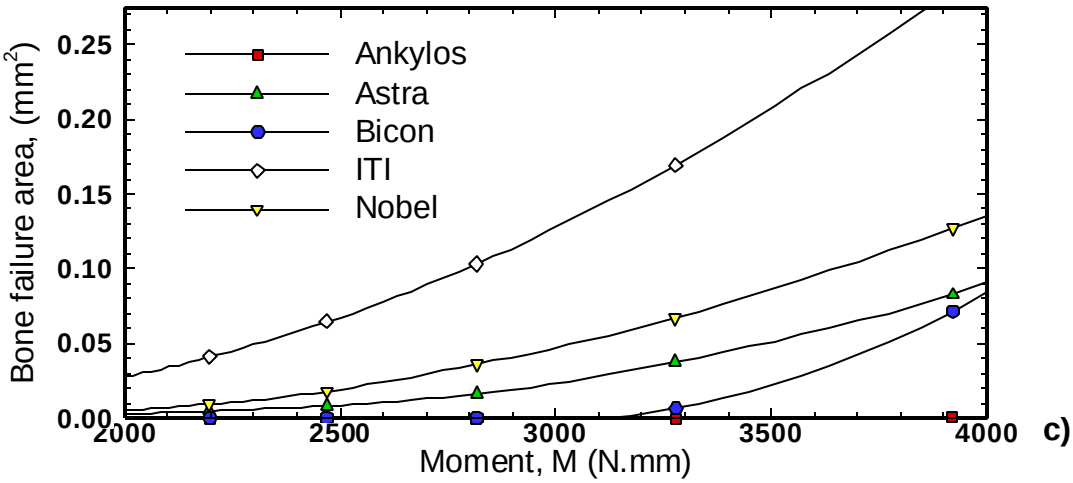

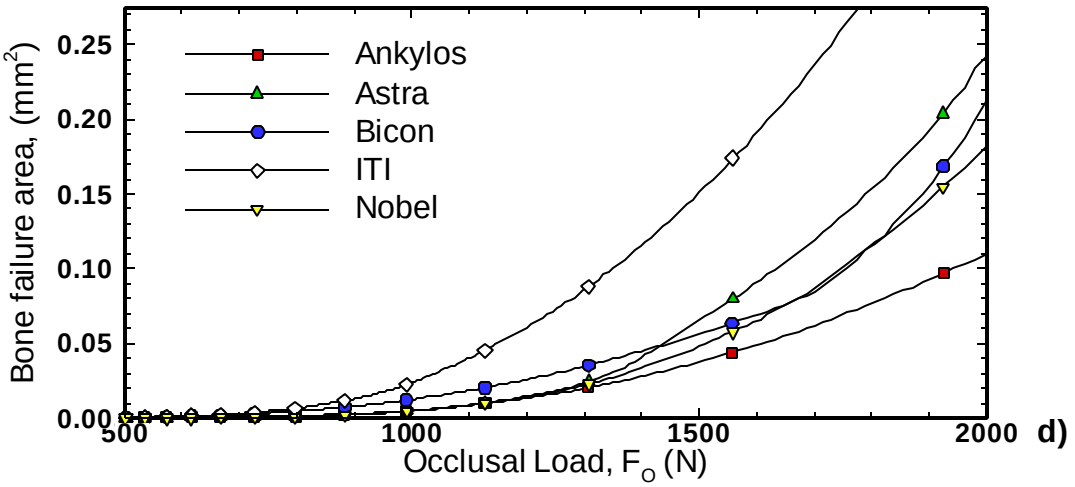

Figure 3. (continued)

Ankylos	Astra	Bicon	ITI	Nobel Biocare
		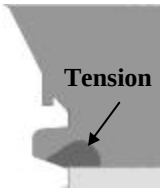	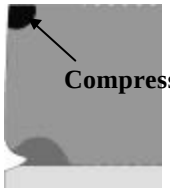	
Bone failure area: 0.134 mm^2 Tension (%): 100	Bone failure area: 0.189 mm^2 Tension (%): 74	Bone failure area: 0.149 mm^2 Tension (%): 100	Bone failure area: 0.268 mm^2 Tension (%): 67	Bone failure area: 0.124 mm^2 Tension (%): 60

a) Vertical force, F_v = 2500 N

				
Bone failure area: 0.006 mm^2 Tension (%): 98	Bone failure area: 0.050 mm^2 Tension (%): 0	Bone failure area: 0.046 mm^2 Tension (%): 46	Bone failure area: 0.213 mm^2 Tension (%): 91	Bone failure area: 0.078 mm^2 Tension (%): 100

b) Lateral force, F_L = 500 N

				
Bone failure area: 0 mm^2 Tension (%): 100	Bone failure area: 0.091 mm^2 Tension (%): 100	Bone failure area: 0.084 mm^2 Tension (%): 100	Bone failure area: 0.305 mm^2 Tension (%): 100	Bone failure area: 0.136 mm^2 Tension (%): 100

c) Bending Moment, M = 4000 N.mm

				
Bone failure area: 0.053 mm^2 Tension (%): 100	Bone failure area: 0.010 mm^2 Tension (%): 46	Bone failure area: 0.073 mm^2 Tension (%): 100	Bone failure area: 0.205 mm^2 Tension (%): 38	Bone failure area: 0.072 mm^2 Tension (%): 13

d) Occlusal force, F_O = 1632 N

Figure 4 Details of the tensile and compressive stress regions which exceed the safe stress limits for a) vertical load, F_V = 2500 N, b) lateral load, F_L = 500 N, c) bending moment, M = 4000 N.mm, and d) occlusal load, F_O = 1632 N.

Implant System	Implant Ref. No	Abutment Ref. No
Ankylos	3101 0053	3102 1100
Astra	22821	
Bicon	260-750-308	260-750-301
ITI	043.241S	048.542
Nobel Biocare	26356	DCA 1028-0

Table 1 The part numbers of the five implant systems and abutments used in the study.

Implant System	Implant Diameter (mm)	Implant Length in the Bone (mm)	Implant Surface Area in the Bone (mm^2)
Ankylos	5.7	8	161.1
Astra	5.4	8.6	187.1
Bicon	5	8.3	228.5
ITI	4.8	8	128.2
Nobel Biocare	5.1	9.4	196.3

Table 2 The geometric properties of the five implant systems used in the study.

Implant System	Number of Elements	Number of Nodes
Ankylos	102,047	102,576
Astra	116,866	120,358
Bicon	92,954	93,229
ITI	91,106	91,510
Nobel Biocare	101,012	101,508

Table 3 The number of elements and nodes used in the finite element models of the five implant systems.